Point by Point Response to Review Comments

Daytime and nighttime aerosol soluble iron formation in clean and slightly-polluted moisture air in a coastal city in eastern China

---

We thank the **Reviewer #2** for the detailed and constructive comments. We provide below point-by-point response to the comments. The reviewer's comments and the original contents of the manuscript are in **black**. The response text is in **blue**. Revisions in the manuscript are in **red**.

General comments:

The manuscript investigated the daytime and nighttime $\%Fe_S$ in $PM_{2.5}$ under clean and SP conditions in a coastal city of China. They found that there was a significant difference between daytime and nighttime $\%Fe_S$ under clean and SP conditions, respectively. Also, they explored the main factors influencing the dissolution of iron, such as aqueous-phase reactions vs. photochemical processes. Although the authors have explored the mechanism of iron dissolution in many ways, the paper suffered from many flaws. For the acidity of the aerosol, this study lacked both constraints of semivolatile gases and a scientific method to verify the accuracy of the simulation results, and thus the authors were very hasty in concluding that aerosols are more acidic, which is very uncritical. In addition, the authors reconstructed $PM_{2.5}$ based on aerosol chemical compositions, which was much higher than $PM_{2.5}$ at nearby station during the same period, is puzzling and suggested that the data in this study may be inaccurate. The authors characterized the relative strength of aerosol acidity, and the use of the $(2[SO_4^{2-}]+[NO_3^-])/PM_{2.5R}$ is incorrect, indicating that the author lacked basic knowledge. The language used in the text is still rough, and it is recommended that the authors strengthen the coherence of the language and simplify redundant expressions. In summary, I do not recommend this article for publication in EGUsphere at present form and it should be returned to the authors for major revision.

General response:

Thanks to the reviewer for the insightful comments. We have implemented the following significant

modifications:

1) We meticulously refined the linguistic expression of the manuscript to enhance precision and brevity.
2) We advanced the methodology for calculating aerosol pH by employing ISORROPIA II. By adopting a stringent condition outlined by Sun et al. (2018), we ensured the stability of our results and further validated the reliability of our aerosol pH calculations through comparisons between model simulations and field observations. We updated all sections pertaining to pH and Ambient Liquid Water Content (ALWC) within the manuscript.
3) We also compared the reconstructed $PM_{2.5}$ (i.e., $PM_{2.5R}$) with the $PM_{2.5}$ data from a nearby monitoring station (i.e., $PM_{2.5S}$), providing thorough explanations for the observed discrepancies between $PM_{2.5R}$ and $PM_{2.5S}$. Moreover, we elaborated the rationality of using the parameter of $(2[SO_4^{2-}] + [NO_3^-])/PM_{2.5R}$ in our work. For more detailed responses and explanations corresponding to the reviewer's comments, please refer to the detailed response to each comment below.

Comment (1): Page 2, line 31-34: Add references including more recent works. For example:

[1] Li, W., Xu, L., Liu, X., Zhang, J., Lin, Y., Yao, X., Gao, H., Zhang, D., Chen, J., and Wang, W., 2017. Air pollution–aerosol interactions produce more bioavailable iron for ocean ecosystems, Sci. Adv., 3, e1601749.

[2] Toner, B.M., 2023. An improved model of the ocean iron cycle. Nature, 620, 41-42.

Response:

We have added the references about recent works as the reviewer suggested on lines 32−35 and 40−42 as follows:

"Its deposition to high-nitrate, low-chlorophyll (HNLC) areas can stimulate phytoplankton boom, and ultimately enhance the absorption and fixation of atmospheric carbon in seawater (Watson et al., 1994; Watson and Lefévre, 1999; Toner, 2023). Studies have shown that only the soluble part of Fe (Fe_S) in aerosols is available to the phytoplankton, namely bioavailable Fe (Zhuang et al., 1992; Sugie et al., 2013; Li et al., 2017)."

"The $\%Fe_S$ in primary particles can be significantly enlarged through atmospheric processes,

which is the consequence of aerosol acidification mainly via aqueous-phase reactions or absorption from the air (Solmon et al., 2009; Shi et al., 2015; Li et al., 2017; Hettiarachchi et al., 2019). ”

Comment (2): Page 2, line 31: It’s not open oceans, exactly, but the HNLC regions.

Response:

We revised the expression on line 32 as follows:

“Its deposition to high-nitrate, low-chlorophyll (HNLC) regions can stimulate phytoplankton boom, and ultimately enhance the absorption and fixation of atmospheric carbon in seawater (Watson et al., 1994; Watson and Lefévre, 1999; Toner, 2023).”

Comment (3): Page 5, line 114: NH_3 is a major alkaline gas in the atmosphere that neutralizes the acidity of aerosols, and the lack of NH_3 will overestimate the acidity of aerosols. How does the author deal with this issue?

Response:

We completely agree with the reviewer that NH_3 plays a significant role in estimating aerosol acidity. In our previous calculation, we included NH_3 during the calculation in ISORROPIAII (version 2.3), utilizing the model in forward-mode. This means we considered both gas data (including HNO_3(g), HCl(g) and NH_3(g)) and aerosol data. The old manuscript line 114 outlined the method for HNO_3(g) calculation, and the method for obtaining HCl(g) and NH_3(g) follows the procedure as that for HNO_3(g). Addressing the reviewer’s concerns regarding the reliability of deriving aerosol pH through only two iterations, we implemented a stringent criterion from Sun et al. (2018) to ensure result stability. Specifically, ISORROPIA was solved iteratively until the change in mass of the output NO_3^- is below 1 %. We provide comprehensive explanations of how we determined the concentrations of HNO_3(g), HCl(g) and NH_3(g) using this approach as follows:

1) Initially, the input of aerosol data was assumed as the sum of aerosol and gas data (specifically for HNO_3, HCl and NH_3). This step yielded both gas and aerosol data from the first run of ISORROPIA.

2) In the second iteration, we added the gas data from the first run to the original aerosol data, and it was considered as the sum of gas data and aerosol data. This combination was treated as the new

input for calculating $HNO_3(g)$, $HCl(g)$ and $NH_3(g)$, similar to the first run.

3) The same procedure was repeated for further iterations until the NO_3^- output variation was less than 1% in mass.

Above calculation processes can be described by the following equations:

$$Input[C_{Aerosol} + C_{Gas}]_{N+1} = C_{Aerosol} + [C_{Gas}]_N$$

$$L = \left| \frac{[C_{NO_3^-}]_{N+1} - [C_{NO_3^-}]_N}{[C_{NO_3^-}]_N} \right| \times 100\%$$

where $C_{Aerosol}$ is the observed concentration of NO_3^- (or NH_4^+, Cl^-); C_{Gas} is the concentration of gaseous species of $HNO_3(g)$ (or $NH_3(g)$, $HCl(g)$); $[C_{Gas}]_N$ is the concentration of gaseous species of $HNO_3(g)$ (or $NH_3(g)$, $HCl(g)$) output by ISORROPIA in the N^{th} run ($N \geq 1$). The iteration was stopped until $L < 1\%$.

After three iterations ($N_{max} = 3$), we determined the newly calculated aerosol pH to be approximately 0.13 units lower than previously calculated. Significant correlations for pH ($r^2 = 0.945$) and ALWC ($r^2 = 0.999$) between the first and the fourth runs confirm the stability and reliability of the pH and ALWC estimations (Figure S2). The calculated $NH_3(g)$ concentration was 2.1 ± 4.0 μg m^{-3}, aligning with observations (mainly ranged from 0 to 8.0 μg m^{-3}) reported by Chen et al. (2021) in Qingdao, 2019. To further validate the ISORROPIA results, we compared the simulated ions against measured values. As demonstrated in Figure S3, the significant correlations for NO_3^- ($R^2 = 0.625$), NH_4^+ ($R^2 = 0.982$) and Cl^- ($R^2 = 0.521$) underscore the high confidence level in the simulation outcomes.

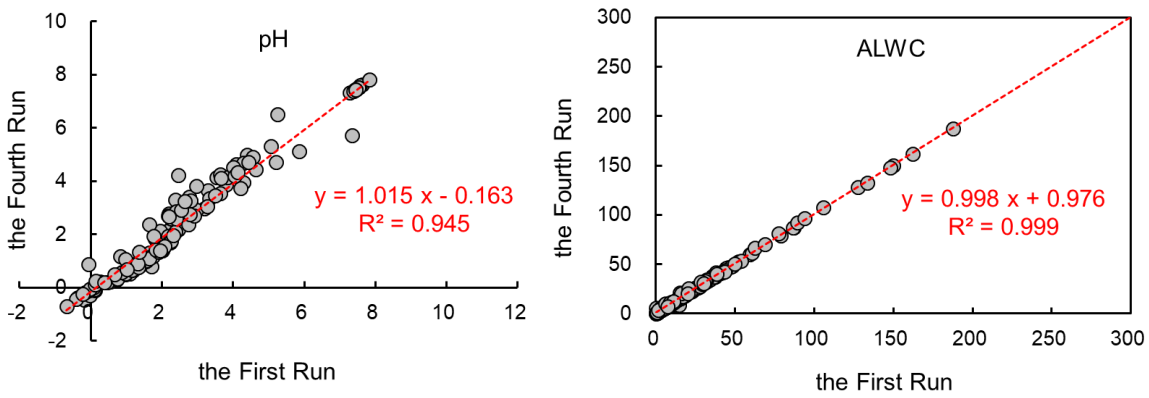

Figure S2: Relationships of aerosol pH and ALWC between the first run and the fourth run of ISORROPIA calculation.

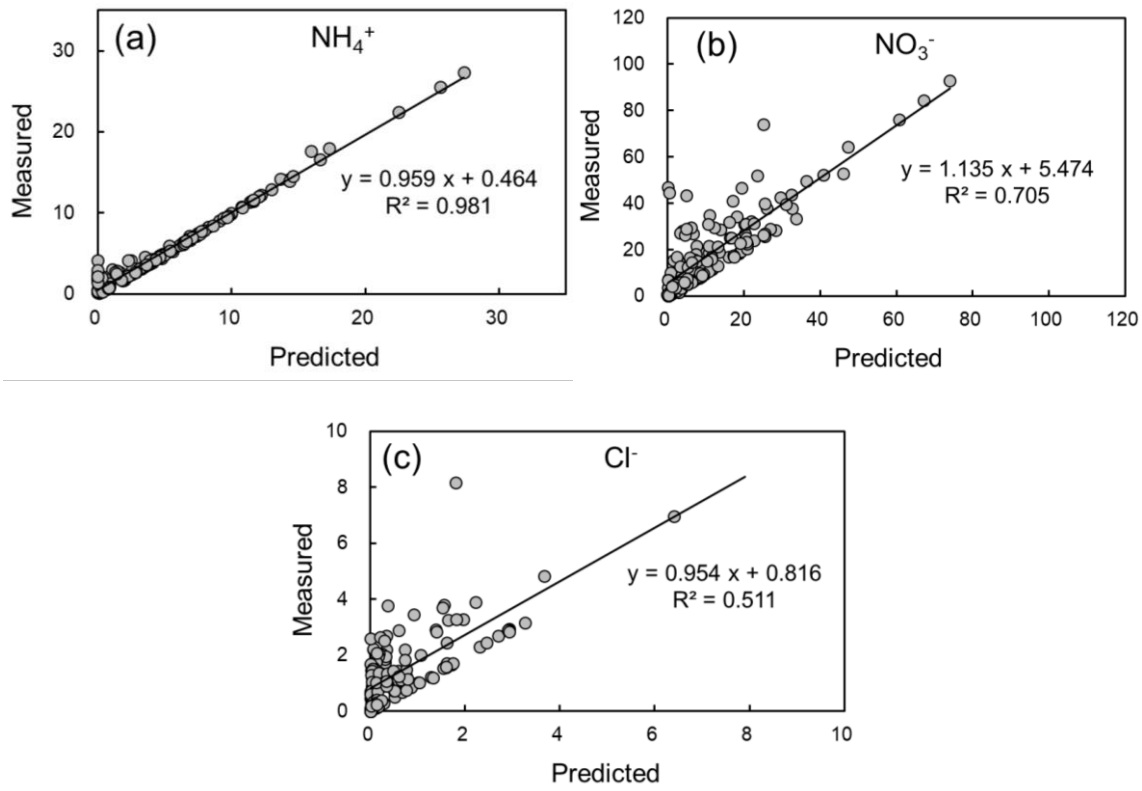

Figure S3: Intercomparisons of simulated and measured concentrations of NO_3^-, NH_4^+ and Cl^-.

The improved method for calculating aerosol pH utilizing ISORROPIA is detailed in Section 2.5 on lines 114–135:

"The concentrations of gaseous species (i.e., $NH_3(g)$, $HNO_3(g)$, HCl(g)) were not measured at the site. In alignment with the approach proposed by Sun et al. (2018), we devised a strategy to estimate the concentrations of these gaseous species. Initially, the input of aerosol data was assumed as the sum of aerosol and gas data (specifically for HNO_3, HCl and NH_3). This step provided us with the first set of gas and aerosol data outputs. For the second run, the gas data output derived from the initial run was added to the original aerosol data, and it was considered as the sum of gas data and aerosol data just like the first run to calculate $HNO_3(g)$, HCl(g) and $NH_3(g)$. The same method was employed for subsequent iterations until the variance in the NO_3^- output below the 1% threshold in mass. The calculation processes can be described by the following equations:

$$Input[C_{Aerosol}+C_{Gas}]_{N+1}=C_{Aerosol}+[C_{Gas}]_N \quad (1)$$

$$L = \left| \frac{[C_{NO_3^-}]_{N+1} - [C_{NO_3^-}]_N}{[C_{NO_3^-}]_N} \right| \times 100\% \quad (2)$$

where $C_{Aerosol}$ is the observed concentration of NO_3^- (or NH_4^+, Cl^-), C_{Gas} is the concentration of gaseous species of $HNO_3(g)$ (or $NH_3(g)$, HCl(g)), and $[C_{Gas}]_N$ is the concentration of gaseous species of $HNO_3(g)$ (or $NH_3(g)$, HCl(g)) output by ISORROPIA in the N^{th} run ($N \geq 1$). The iteration was stopped until L < 1%.

Finally, three times of iterations ($N_{max} = 3$) were determined when L = 0.1%. The aerosol pH was calculated by using aqueous H^+ concentration and aerosol liquid water content (ALWC) outputted by ISORROPIA, as described by equation (3).

$$pH = -\log_{10} \frac{1000 \times H^+(aq)}{ALWC} \quad (3)$$

Significant correlations between the results of the first run and the fourth run were observed for pH ($r^2 = 0.95$) and ALWC ($r^2 = 0.99$), indicating the stability and reliability in estimating the pH and ALWC by ISORROPIA II (Figure S2). Moreover, the correlations of NO_3^- ($r^2 = 0.71$), NH_4^+ ($r^2 = 0.98$) and Cl^- ($r^2 = 0.51$) between the simulated results and measured concentrations are significant, demonstrating the robust confidence level of the simulated results (Figure S3)."

References

Chen, D., Shen, Y., Wang, J., Gao, Y., Gao, H., and Yao, X.: Mapping gaseous dimethylamine, trimethylamine, ammonia, and their particulate counterparts in marine atmospheres of China's marginal seas – Part 1: Differentiating marine emission from continental transport, Atmos. Chem. Phys., 21, 16413-16425, 10.5194/acp-21-16413-2021, 2021.

Sun, P., Nie, W., Chi, X., Xie, Y., Huang, X., Xu, Z., Qi, X., Xu, Z., Wang, L., Wang, T., Zhang, Q., and Ding, A.: Two years of online measurement of fine particulate nitrate in the western Yangtze River Delta: influences of thermodynamics and N2O5 hydrolysis, Atmos. Chem. Phys., 18, 17177-17190, 10.5194/acp-18-17177-2018, 2018.

Comment (4): Line 119: Equation 1: here, the authors only calculated aerosol acidity for inorganic ions? What about organic acids? The authors measured organic acids, so how was the contribution of

organic acids calculated? The contribution of organic matter should be added.

Response:

The impact of organic matter (OM) on aerosol pH was determined to be minimal. This can be attributed to the limited sensitivity of the predicted pH to the water uptake by organic species ($ALWC_{org}$) when the OM fraction in $PM_{2.5}$ is low (Guo et al., 2015). For instance, Liu et al. (2017) found that in Beijing, the $ALWC_{org}$ constituted merely 5% of the total ALWC, during which the organic matter constituted approximately 30% of the daily $PM_{2.5}$ mass, signifying its negligible impact on aerosol acidity. Consequently, they omitted the consideration of particle water associated with organic aerosol mass in their aerosol pH calculation. This methodological approach was similarly adopted by Ding et al. (2019) and Zhang et al. (2022). In our study, the proportions of OM in $PM_{2.5}$ during clean and the SP periods were ~11.9% and ~15.7%, respectively, markedly lower than the proportion reported by Liu et al. (2017). Moreover, the mass fractions of water-soluble ions (WSIs) in $PM_{2.5}$ during these periods were ~74.6% and ~72.5%, respectively, suggesting that WSIs were the predominant constituents in $PM_{2.5}$ mass. Hence, it can be inferred that the influence of OM on aerosol pH was inconsequential.

To validate our viewpoint, we assessed the contribution of OM on aerosol pH, employing the same method delineated by Guo et al. (2015) to calculate $ALWC_{org}$ as the following equation:

$$ALWC_{org} = \frac{m_{org}\rho_w}{\rho_{org}} \frac{\kappa_{org}}{(\frac{100\%}{RH} - 1)}$$

where m_{org} is the OM concentration, estimated as 1.6 times the OC concentration (Turpin and Lim, 2001), ρ_w is water density (1.0×10^3 kg m^{-3}), and a typical organic density (ρ_{org}) of 1.4×10^3 kg m^{-3} was used. κ_{org} is the hygroscopicity parameter of organic aerosol compositions. We did not observe κ_{org} during the campaign, so we adopted a typical range of 0.05−0.20 (Kuang et al., 2020). In Beijing, the typical κ_{org} of 0.06 was used in previous studies (Cheng et al., 2016). The parameter's magnitude directly influences the calculated $ALWC_{org}$, with higher κ_{org} values resulting in greater $ALWC_{org}$. Our analysis determined the $ALWC_{org}$ to range between 0.83 and 3.31 μg m^{-3}, constituting merely 2.6−9.8% of the total ALWC. The aerosol pH was about 2.49 without considering OM, adjusting to a range of 2.52−2.57 upon considering OM, thus affirming the negligible effect of OM on aerosol pH.

In summary, the negligible influence of OM on aerosol pH rationalizes the exclusion of OM's contribution to ALWC from the data analysis of this study. We have expanded upon this discussion in the revised manuscript on lines 136−142 and supporting information in Text S1:

"In addition, the impact of organic matter (OM) on aerosol pH was determined to be minimal. This can be attributed to the limited sensitivity of the predicted pH to the water uptake by organic species ($ALWC_{org}$) when the OM fraction in $PM_{2.5}$ is low (Guo et al., 2015; Liu et al., 2017). Following the methods of Guo et al. (2015), we estimated $ALWC_{org}$ and its influence on aerosol pH. Our analysis determined the $ALWC_{org}$ to range between 0.83 and 3.31 μg m^{-3}, constituting merely 2.6−9.8% of the total ALWC. Aerosol pH was about 0.03−0.08 higher when considering OM, thus affirming the negligible effect of OM on aerosol pH (see Text S1 in the supporting information for more details)."

"**Text S1. The influence of organic matters on aerosol pH**

We utilized the same method of Guo et al. (2015) to calculated $ALWC_{org}$ as the following equation:

$$ALWC_{org} = \frac{m_{org}\rho_w}{\rho_{org}} \frac{\kappa_{org}}{(\frac{100\%}{RH} - 1)}$$

where m_{org} is the OM concentration, which was estimated with 1.6 times OC (Turpin and Lim, 2001), ρ_w is water density (1.0×10^3 kg m^{-3}), and a typical organic density (ρ_{org}) of 1.4×10^3 kg m^{-3} was used. κ_{org} is the hygroscopicity parameter of organic aerosol compositions. We did not observe κ_{org} during the campaign, so we applied a typical range of 0.05−0.20 (Kuang et al., 2020). In Beijing, the typical κ_{org} of 0.06 was used in previous studies (Cheng et al., 2016). The higher the κ_{org} is, the larger the $ALWC_{org}$ would be. At last, we evaluated the range of $ALWC_{org}$ as 0.83−3.31 μg m^{-3}, which only accounted for 2.6−9.8% of the total ALWC. pH was about 2.49 without considering OM, and it was 2.52−2.57 when considering OM, indicating that the influence of OM in aerosol pH was very weak."

References

Cheng, Y. F., Zheng, G. J., Wei, C., Mu, Q., Zheng, B., Wang, Z. B., Gao, M., Zhang, Q., He, K. B., Carmichael, G., Poschl, U., and Su, H.: Reactive nitrogen chemistry in aerosol water as a source of sulfate during haze events in China, Sci. Adv., 2, 11, 10.1126/sciadv.1601530, 2016.

Ding, J., Zhao, P., Su, J., Dong, Q., Du, X., and Zhang, Y.: Aerosol pH and its driving factors in Beijing, Atmos. Chem. Phys., 19, 7939-7954, 10.5194/acp-19-7939-2019, 2019.

Guo, H., Xu, L., Bougiatioti, A., Cerully, K. M., Capps, S. L., Hite Jr, J. R., Carlton, A. G., Lee, S. H., Bergin, M. H., Ng, N. L., Nenes, A., and Weber, R. J.: Fine-particle water and pH in the southeastern United States, Atmos. Chem. Phys., 15, 5211-5228, 10.5194/acp-15-5211-2015, 2015.

Kuang, Y., Xu, W., Tao, J., Ma, N., Zhao, C., and Shao, M.: A Review on Laboratory Studies and Field Measurements of Atmospheric Organic Aerosol Hygroscopicity and Its Parameterization Based on Oxidation Levels, Current Pollution Reports, 6, 410-424, 10.1007/s40726-020-00164-2, 2020.

Liu, M., Song, Y., Zhou, T., Xu, Z., Yan, C., Zheng, M., Wu, Z., Hu, M., Wu, Y., and Zhu, T.: Fine particle pH during severe haze episodes in northern China, Geophys. Res. Lett., 44, 5213-5221, https://doi.org/10.1002/2017GL073210, 2017.

Turpin, B. J. and Lim, H.-J.: Species Contributions to PM2.5 Mass Concentrations: Revisiting Common Assumptions for Estimating Organic Mass, Aerosol Science and Technology, 35, 602-610, 10.1080/02786820119445, 2001.

Zhang, H., Li, R., Dong, S., Wang, F., Zhu, Y., Meng, H., Huang, C., Ren, Y., Wang, X., Hu, X., Li, T., Peng, C., Zhang, G., Xue, L., Wang, X., and Tang, M.: Abundance and Fractional Solubility of Aerosol Iron During Winter at a Coastal City in Northern China: Similarities and Contrasts Between Fine and Coarse Particles, Journal of Geophysical Research: Atmospheres, 127, e2021JD036070, https://doi.org/10.1029/2021JD036070, 2022.

Comment (5): Line 120-122: For ISORROPIA simulations, good results after two iterations of validation do not imply that ISORROPIA is able to accurately calculate the pH of the aerosol, which depends on the concentration of semi-volatile gases and ionic components. In addition, the goodness of model simulation results is usually assessed by minimizing the difference between simulated ions and gases and measured values, as detailed in Guo et al. 2017 and Song et al., 2018.

References:

[1] Guo, H., Liu, J., Froyd, K. D., Roberts, J. M., Veres, P. R., Hayes, P. L., Jimenez, J. L., Nenes, A., and Weber, R. J.: Fine particle pH and gas–particle phase partitioning of inorganic species in Pasadena, California, during the 2010 CalNex campaign, Atmos. Chem. Phys., 17, 5703–5719, https://doi.org/10.5194/acp-17-5703-2017.

[2] Song, S., Gao, M., Xu, W., Shao, J., Shi, G., Wang, S., Wang, Y., Sun, Y., and McElroy, M. B.:

Fine-particle pH for Beijing winter haze as inferred from different thermodynamic equilibrium models, Atmos. Chem. Phys., 18, 7423–7438, https://doi.org/10.5194/acp-18-7423-2018.

Response:

To enhance the reliability of the method, we adopted a restrictive condition utilized by Sun et al. (2018) to ensure the stability of the results, i.e., ISORROPIA was solved iteratively until output NO_3^- changed by < 1 % in mass. The goodness of model simulations was also assessed by comparing the difference between simulated ions and the measured values to demonstrate the reliability of the results obtained by ISORROPIA calculation. Detailed results are shown in the response of **Comment (3)**.

Comment (6): Line 131: Equation 2, The authors performed a mass reconstruction of $PM_{2.5}$, which needs to be compared with $PM_{2.5}$ from nearby monitoring stations to demonstrate the validity of this approach, at least in terms of trends. In addition, as can be seen in Table 1, the sum of the components of $PM_{2.5}$ at each stage exceeds the $PM_{2.5}$ concentration observed at the nearby ambient monitoring station, so why is there such a big difference? According to the data provided by the authors, the reconstructed $PM_{2.5}$ = 33.47 was calculated, which is almost twice as much as that of the nearby monitoring station. The difference is so obvious at such a close distance that the authors firstly need to ensure the accuracy of the data before the next analysis.

Response:

The comparison between the reconstructed $PM_{2.5}$ (i.e., $PM_{2.5R}$) with the $PM_{2.5}$ reported from an adjacent monitoring station (i.e., $PM_{2.5S}$) revealed congruent variation trends between these datasets, as depicted in Figure R3a, indicating the high confidence of the $PM_{2.5R}$ dataset.

However, we also noticed that the level of $PM_{2.5R}$ is higher than the $PM_{2.5S}$ observed from the nearby monitoring station. As shown in Figure R3b, the disparity between $PM_{2.5R}$ and $PM_{2.5S}$, expressed as the ratios of the difference to $PM_{2.5S}$ (i.e., $(PM_{2.5R} - PM_{2.5S})/PM_{2.5S}$), predominantly spans from 0.3 to 3.1, averaging at 1.7. This discrepancy is hypothesized to emanate predominantly from two reasons:

1) The geographical disparity between these two observation locations. Figure S1 elucidates that the monitoring station (depicted as a yellow dot) is situated approximately 4.6 km to the southwest of the sampling site, nestled closer to the sea and further away from human activity areas. Therefore, the chosen standard monitoring station avoided the influence from anthropogenic activities to a large

extent, thereby accounting for the higher $PM_{2.5R}$ concentrations compared to $PM_{2.5S}$.

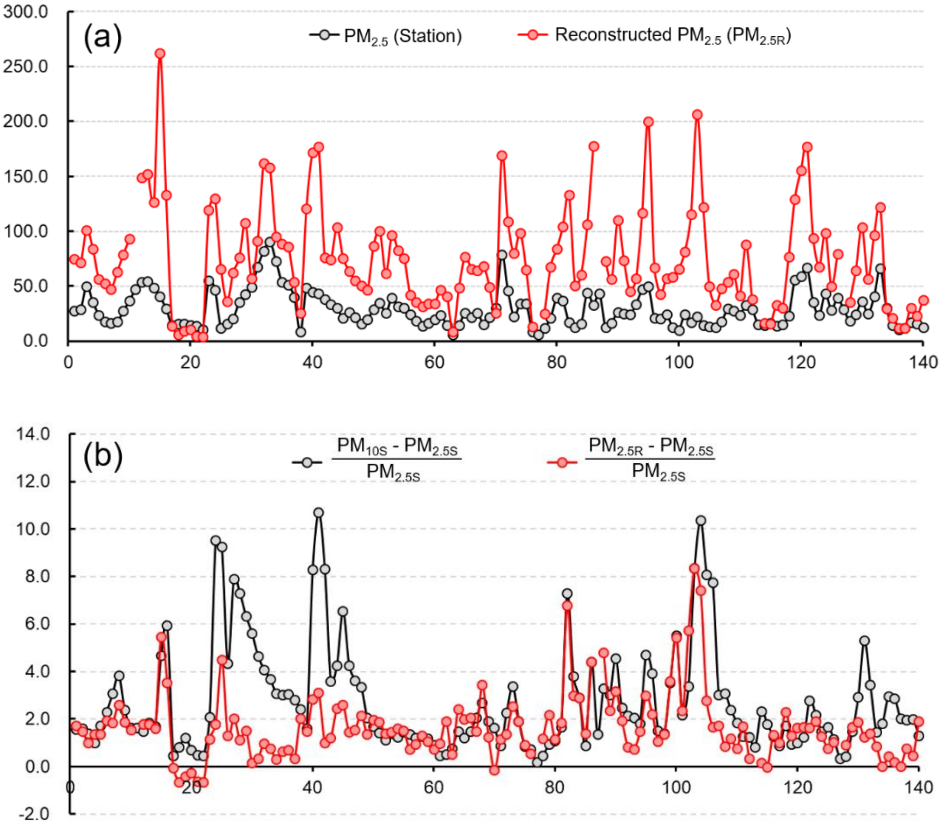

Figure R3: Variations of $PM_{2.5}$ concentrations (a) and comparative parameters (b) during the sampling period. The x-axis shows the sample number. The black and red lines in (a) stand for the $PM_{2.5}$ concentrations obtained from a nearby monitoring station (i.e., $PM_{2.5S}$) and reconstructed $PM_{2.5}$ (i.e., $PM_{2.5R}$), respectively. The black line in (b) shows the ratios of the difference of PM_{10S} and $PM_{2.5S}$ to $PM_{2.5S}$, indicating the degree of difference between $PM_{2.5}$ and PM_{10}. The red line in (b) shows the ratios of the difference of $PM_{2.5R}$ and $PM_{2.5S}$ to $PM_{2.5S}$, indicating the degree of difference between the reconstructed $PM_{2.5}$ and the $PM_{2.5}$ observed by the monitoring station.

2) Different sampling instruments and the influence of coarse particles. Even though the capture efficiencies of the sampler cutting heads ($PM_{2.5}$ cyclone) for $PM_{2.5}$ of these two sites were same. i.e., 50%, the models and specifications of the instruments used at these two sites were different. This means that the geometric standard deviations of sampling efficiency may be different. The geometric standard deviation of sampling efficiency is usually expressed as the ratio of the particle aerodynamic diameter (D_{a50}) corresponding to a capture efficiency of 50% to the particle aerodynamic diameter (D_{a84}) corresponding to a capture efficiency of 84%. If the geometric standard deviations of sampling efficiency of two sampling instruments are different, then their capture efficiencies for coarse particles (e.g., PM_{10}) will be different. It may result in a noticeable difference in observed fine particles, because

the mass of atmospheric particulate matter is mainly concentrated in coarse particles. We compared the ratio of (PM_{10S} - $PM_{2.5S}$)/$PM_{2.5S}$ with the ratio of ($PM_{2.5R}$ - $PM_{2.5S}$)/$PM_{2.5S}$ and found a high degree of consistency between them (Figure R3b). In other words, the higher the proportion of coarse particles in the atmosphere, the greater the difference between of $PM_{2.5R}$ and $PM_{2.5S}$. Significant differences usually occur when the proportion of coarse particles is high, mainly during the dust-influenced periods. But this study focused on clean and the SP periods, so absurd difference barely occur.

We added more explanations about this issue on lines 156−158:

"Because the nearby monitoring station is closer to the sea and less affected by human activities (yellow dot in Figure S1), the level of $PM_{2.5R}$ is higher than the observations from the monitoring station. But the trends of variations of these two datasets were consistent, indicating the high confidence of the $PM_{2.5R}$ dataset."

Comment (7): Line 158-160: Table 1, the calculated pHs are very low, indicating that the aerosols are strongly acidic. However, according to Wang et al., 2022, aerosols in the northern offshore are weakly acidic, and the pH of the aerosols in this study is much higher than that in the literature, which I think is most likely caused by the lack of data on NH_3, and therefore the pH calculated by the authors here lacks credibility. I suggest that the authors include data on NH_3 from the same period, or find data on atmospheric NH_3 concentration in Qingdao from previous literature.

References:

[1] Wang, G., Tao, Y., Chen, J., Liu, C., Qin, X., Li, H., Yun, L., Zhang, M., Zheng, H., Gui, H., Liu, J., Huo, J., Fu, Q., Deng, C., Huang, K*., 2022. Quantitative Decomposition of Influencing Factors to Aerosol pH Variation over the Coasts of the South China Sea, East China Sea, and Bohai Sea. Environmental Science & Technology Letters, 9(10), 815–821, https://doi.org/10.1021/acs.estlett.2c00527.

Response:

In our calculation using ISORROPIA, gaseous ammonia $NH_3(g)$ was duly accounted for. We elaborated on the method of retrieving $NH_3(g)$ in detail in the response of **Comment (3)**, and found that the concentrations of $NH_3(g)$ were 2.1 ± 4.0 μg m^{-3} output by ISORROPIA, aligning with the

observations (mainly ranged from 1 to 8 μg m^{-3}) reported by Chen et al. (2021) in Qingdao during the year 2019. Moreover, the correlation between simulated NH_4^+ and measured concentrations is statistically significant (r^2 = 0.982, Figure S3), endorsing the simulated results with a high degree of confidence. The aerosol pH estimated through a more rigorous iterative method shows only minor variations compared to the results of the previous manuscript, with a difference of merely about 0.13.

Even though the aerosol pH values calculated by Wang et al. (2022) are higher than those observed in our study, it is important to note that the locations of sampling sites, seasons and years of respective studies varied significantly. Consequently, substantial differences in atmospheric conditions (e.g., relative humidity and temperature) and chemical compositions of aerosols are expected. Moreover, Figure R4 presented in the article by Wang et al. (2022) supports the conclusion that extremely low pH levels in coastal areas, such as Tanggu (with a pH approximated at 1.3) and the Bohai Sea (with a pH around 1.2), are plausible. This is attributed to the scarcity of alkaline substance sources (e.g., NH_3) over the oceanic regions (Zhou et al., 2018).

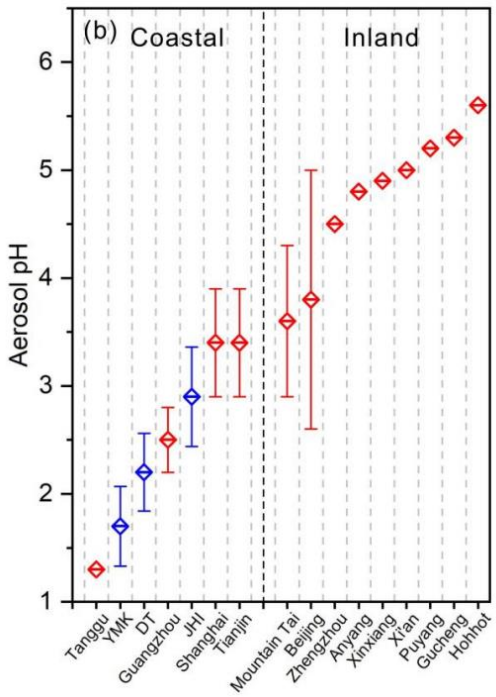

Figure R4 Comparison of aerosol pH among various coastal and inland sites of China, which was reported by Wang et al. (2022).

In our work, episodes of extreme aerosol pH were documented during the clean period. During the clean period, the air masses primarily originated from sea areas, leading to significantly acidic aerosol pH due to the absence of alkaline substance sources. In addition, throughout the entire

campaign, the calculated aerosol pH did not drop drastically, maintaining an average of around 2.5, including during clean, SP, heavily-polluted, fog-influenced, and dust-related periods.

On another note, the pronounced aerosol acidity observed in our work was mainly induced by the elevated proportions of SO_4^{2-} and NO_3^- in $PM_{2.5}$, resulting in a low level of ion balance (IB). The IB and equivalent ratios were calculated using the following equations, utilizing the charge-equivalent measured ion concentrations:

$$IB=[Anions]-[Cations]$$

$$[Anions]=\frac{[SO_4^{2-}]}{96}\times 2+\frac{[NO_3^-]}{62}+\frac{[Cl^-]}{35.5}+\frac{[C_2O_4^{2-}]}{88}\times 2+\frac{[F^-]}{19}$$

$$[Cations]=\frac{[Na^+]}{23}+\frac{[NH_4^+]}{18}+\frac{[K^+]}{39}+\frac{[Mg^{2+}]}{24}\times 2+\frac{[Ca^{2+}]}{40}\times 2$$

where [cations] and [anions] are the sum of charge-equivalent total molar concentrations (μmol m^{-3}) of cations and anions, respectively; $[Na^+]$, $[NH_4^+]$, $[K^+]$, $[Mg^{2+}]$, $[Ca^{2+}]$, $[SO_4^{2-}]$, $[NO_3^-]$, $[Cl^-]$, $[C_2O_4^{2-}]$ and $[F^-]$ are the mass concentrations (μg m^{-3}) of these ions in the atmosphere. In our work, IB mainly ranged from −0.01 μmol m^{-3} to 0.25 μmol m^{-3} during the clean period and from 0.04 μmol m^{-3} to 0.51 μmol m^{-3} during the SP period. The low IB facilitated enhanced $[H^+]$ levels, contributing to the low observed pH. These results align with the phenomena documented by Guo et al. (2015), where aerosol pH levels were typically below 1 in scenarios where the IB exceeded 0.05 μmol m^{-3} (Figure R5). This can also support the rationality of our aerosol acidity.

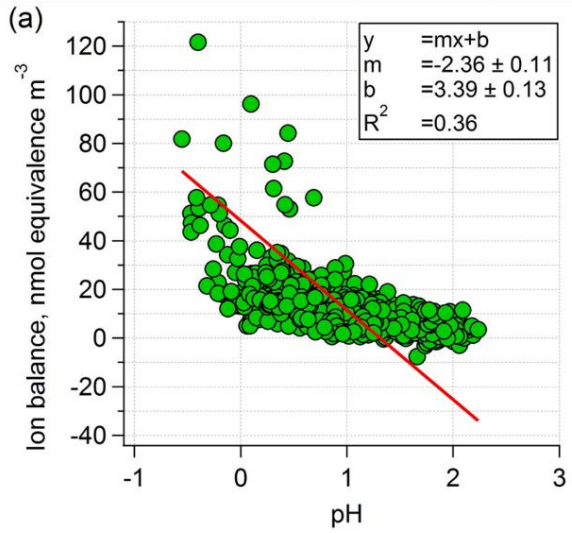

Figure R5 Comparison of ion balance with pH as provided by Guo et al. (2015).

In the revision, we conducted more discussions on this issue on lines 215–222:

"The aerosol pH calculated in this work was evidently lower than many other areas of China (Liu et al., 2017; Wang et al., 2019; Xu et al., 2020). During the clean period, air masses mainly originated from the seas. Therefore, the aerosol pH can be very acidic because of the lack of sources of alkaline substances over the ocean, such as NH_3, Ca^{2+}, et al. (Zhou et al., 2018). Compared to the inland areas, much lower aerosol pH in coastal areas is reasonable (Wang et al., 2022). For instance, Zhou et al. (2018) reported that the pH of aerosols near the Bohai Sea can be as low as around 1.0. Moreover, they also found that the daytime aerosol acidity was significantly stronger than that during the nighttime in coastal areas. This observation aligns with the findings during clean periods in our study, which were characterized by the predominance of sea breezes."

References

Chen, D., Shen, Y., Wang, J., Gao, Y., Gao, H., and Yao, X.: Mapping gaseous dimethylamine, trimethylamine, ammonia, and their particulate counterparts in marine atmospheres of China's marginal seas – Part 1: Differentiating marine emission from continental transport, Atmos. Chem. Phys., 21, 16413-16425, 10.5194/acp-21-16413-2021, 2021.

Guo, H., Xu, L., Bougiatioti, A., Cerully, K. M., Capps, S. L., Hite Jr, J. R., Carlton, A. G., Lee, S. H., Bergin, M. H., Ng, N. L., Nenes, A., and Weber, R. J.: Fine-particle water and pH in the southeastern United States, Atmos. Chem. Phys., 15, 5211-5228, 10.5194/acp-15-5211-2015, 2015.

Liu, M., Song, Y., Zhou, T., Xu, Z., Yan, C., Zheng, M., Wu, Z., Hu, M., Wu, Y., and Zhu, T.: Fine particle pH during severe haze episodes in northern China, Geophys. Res. Lett., 44, 5213-5221, https://doi.org/10.1002/2017GL073210, 2017.

Wang, G., Tao, Y., Chen, J., Liu, C., Qin, X., Li, H., Yun, L., Zhang, M., Zheng, H., Gui, H., Liu, J., Huo, J., Fu, Q., Deng, C., and Huang, K.: Quantitative Decomposition of Influencing Factors to Aerosol pH Variation over the Coasts of the South China Sea, East China Sea, and Bohai Sea, Environmental Science & Technology Letters, 9, 815-821, 10.1021/acs.estlett.2c00527, 2022.

Wang, H., Ding, J., Xu, J., Wen, J., Han, J., Wang, K., Shi, G., Feng, Y., Ivey, C. E., Wang, Y., Nenes, A., Zhao, Q., and Russell, A. G.: Aerosols in an arid environment: The role of aerosol water content, particulate acidity, precursors, and relative humidity on secondary inorganic aerosols,

Science of The Total Environment, 646, 564-572, https://doi.org/10.1016/j.scitotenv.2018.07.321, 2019.

Xu, J., Chen, J., Zhao, N., Wang, G., Yu, G., Li, H., Huo, J., Lin, Y., Fu, Q., Guo, H., Deng, C., Lee, S. H., Chen, J., and Huang, K.: Importance of gas-particle partitioning of ammonia in haze formation in the rural agricultural environment, Atmos. Chem. Phys., 20, 7259-7269, 10.5194/acp-20-7259-2020, 2020.

Zhou, M., Zhang, Y., Han, Y., Wu, J., Du, X., Xu, H., Feng, Y., and Han, S.: Spatial and temporal characteristics of PM2.5 acidity during autumn in marine and coastal area of Bohai Sea, China, based on two-site contrast, Atmos. Res., 202, 196-204, https://doi.org/10.1016/j.atmosres.2017.11.014, 2018.

Comment (8): Line 163-164, line 182: Here the authors are advised to use the reconstructed $PM_{2.5}$ mass.

Response:

In this study, the primary purpose of using the $PM_{2.5}$ reported from the monitoring station (i.e., $PM_{2.5S}$) was to classify cases into either 'clean' or 'SP' instances based on air quality. Due to the multitude of issues and difficulties associated with weighing high-volume sample collections, we did not perform mass concentration weighing and PM mass concentration calculation. To ensure that this classification criterion is comparable in other studies, and considering that reconstructed $PM_{2.5}$ (i.e., $PM_{2.5R}$) is only an estimated value of partial components with some uncertainties, we believe it is more appropriate to use $PM_{2.5S}$ data from national standard monitoring stations on lines 163−164 (old manuscript).

In terms of the contents on line 182 (old manuscript), the data presented were initially derived by using $PM_{2.5R}$. The proportions of chemical species in $PM_{2.5}$ in this study were calculated by dividing the concentration of chemical species by $PM_{2.5R}$. We have added further clarification in the manuscript on lines 158−160 to more clearly articulate this issue:

"In addition, any mention of ionic ratios or normalized parameters in the results and discussions of this paper indicates the data was divided by $PM_{2.5R}$."

Comment (9): Line 165: What are degraded air conditions? In general, atmospheric boundary layer

heights are higher during the day and lower at night, and here the authors' assertion that the higher Fe_T and Fe_S during the day are due to degraded atmospheric diffusion conditions lacks conclusive evidence. It is also possible that this is facilitated by stronger photochemical processes during the day.

Response:

The previous statement was not accurately phrased. The intention was to suggest that the elevated daytime values of Fe_T and Fe_S might be associated with higher aerosol pollution due to increased human activities. However, there isn't a significant difference between daytime and nighttime $PM_{2.5}$ values (16.9 vs. 16.4 μg m^{-3}). As the reviewer pointed out, the atmospheric boundary layer during the day is higher than at night, leading to more favorable dispersion conditions, which might contribute to the minimal diurnal variation in PM levels. Daytime human activities are more intense, and this too could be a reason for the higher daytime concentrations of both Fe_T and Fe_S. Another possibility, as highlighted by the reviewer, is that daytime photochemical processes could lead to higher concentrations of Fe_S. Taking these points into consideration, we have reorganized the logic and made the following revision on lines 184–189:

"Compared to the nighttime, Fe_T and Fe_S concentrations were higher during the daytime, which were 289.2 ± 223.4 ng m^{-3} and 20.0 ± 10.5 ng m^{-3}, respectively. Daytime levels of Fe_T and Fe_S were 1.5 times and 1.6 times as high as those observed at night, respectively. The increase in Fe_T and Fe_S during daytime may be linked to heightened human activities. Furthermore, the elevated Fe_S during daytime could be attributed to photochemical processes, which promoted the dissolution of aerosol Fe, a topic to be discussed further in Section 4.2."

Comment (10): Line 187-190: The use of $(2[SO_4^{2-}]+[NO_3^-])/PM_{2.5R}$ to characterize the level of acidity in a unit of $PM_{2.5}$ is erroneous; the acidity of the aerosol, however, is determined by the amount of H^+ in the aqueous system, which is determined by the combination of acids and bases in the aerosol system.

Response:

We agree with the reviewers that $(2[SO_4^{2-}] + [NO_3^-])/PM_{2.5R}$ does not signify the acidity of aerosols. Instead, our use of this parameter aims to denote the proportion of acidic substances contained within a unit mass of particulate matter. Because sulfate and nitrate were dominant acidic species in WSIs

(constituting >75% of the mass) in this study and both of them are strong acids, the quantity of acidic substances in $PM_{2.5}$ can be evaluated through $(2[SO_4^{2-}] + [NO_3^-])/PM_{2.5R}$. Figure 3a proves that the significant dependence of pH on $(2[SO_4^{2-}]+[NO_3^-])/PM_{2.5R}$, elucidating that SO_4^{2-} and NO_3^- played dominant roles in driving aerosol pH. We also pinpointed possible mechanisms that caused this phenomenon in the manuscript. We have further clarified this issue on lines 222−224 as follows:

"In this study, we employed the ratio of acidic substances to PM, namely, $(2[SO_4^{2-}] + [NO_3^-])/PM_{2.5R}$, to characterize the level of acidic substances in a unit of $PM_{2.5}$, because SO_4^{2-} and NO_3^- were predominant acidic species within WSIs (>75% in mass)."

The dependence of pH on $(2[SO_4^{2-}] + [NO_3^-] - [NH_4^+])/PM_{2.5R}$ was also studied as shown in Figure R6. The dependence of pH on $(2[SO_4^{2-}] + [NO_3^-] - [NH_4^+])/PM_{2.5R}$ was far less significant than on $(2[SO_4^{2-}] + [NO_3^-])/PM_{2.5R}$, indicating the critical roles of SO_4^{2-} and NO_3^- in regulating the aerosol pH.

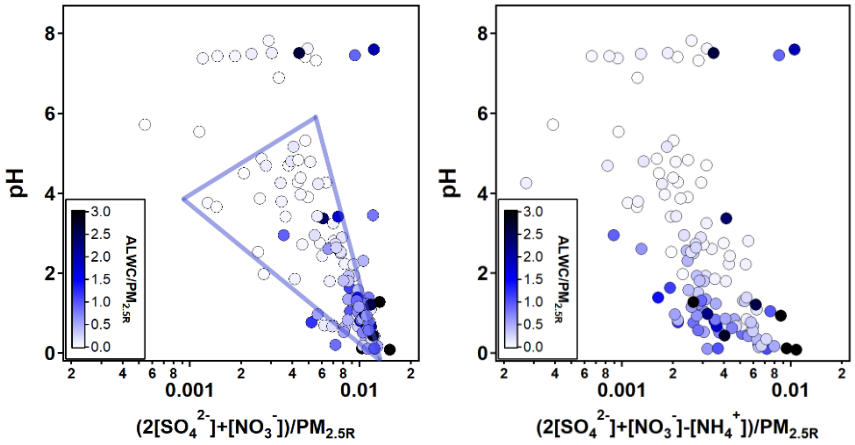

Figure R6: Dependence aerosol pH on $(2[SO_4^{2-}] + [NO_3^-])/PM_{2.5R}$ (left) and $(2[SO_4^{2-}] + [NO_3^-] - [NH_4^+])/PM_{2.5R}$ (right) during the whole sampling period. Circles are colored by $ALWC/PM_{2.5R}$ (unit: μg $μg^{-1}$).

Comment (11): Line 199-203: Why are the authors' calculated daytime and nighttime aerosol pH values so large for different pollution scenarios when the SNA percentages are close? During the cleaning period, daytime pH is lower than nighttime, and during the pollution period is nighttime lower than daytime?

Response:

We explained this issue by using the relationships between pH and $(2[SO_4^{2-}] + [NO_3^-])/PM_{2.5R}$ on lines 256–260 in Section 4.1:

"Especially during clean and SP periods (r = 0.62, Figure 3a), the slope of the regression line was approximately –602.99, indicating that a variation of 1.0 nmol μg^{-1} of the acidic species content in $PM_{2.5}$ can lead to a noticeable fluctuation of aerosol pH (about 0.60). For instance, the daytime aerosol pH was 0.60 lower than that of the nighttime during the clean period, even though the difference of the two acidic species content was only about 1.0 nmol μg^{-1}."

Actually, a variation of 1.0 nmol μg^{-1} of $(2[SO_4^{2-}]+[NO_3^-])/PM_{2.5R}$ is far from being minor. We evaluated the pH variation, i.e., ΔpH, caused by a fluctuation of 1.0 nmol μg^{-1} of $(2[SO_4^{2-}]+[NO_3^-])/PM_{2.5R}$. Assuming the NH_4^+ concentration is stable, an increase of $(2[SO_4^{2-}]+[NO_3^-])/PM_{2.5R}$ of 1.0 nmol μg^{-1} indicates an $[H^+]$ increase of 1.0 nmol μg^{-1}. The resulting pH variation can be calculated by the following equation:

$$\begin{aligned}\Delta pH &= pH_{original} - pH_{present} = lg[H^+]_{present} - lg[H^+]_{original} \\ &= lg\frac{n(H^+)_{original} + \Delta n(H^+)}{ALWC_{original}} - lg\frac{n(H^+)_{original}}{ALWC_{original}} \\ &= lg\left(\frac{n(H^+)_{original} + \Delta n(H^+)}{ALWC_{original}} \times \frac{ALWC_{original}}{n(H^+)_{original}}\right) = lg\frac{n(H^+)_{original} + \Delta n(H^+)}{n(H^+)_{original}} \\ &= lg\left(1 + \frac{\Delta n(H^+)}{n(H^+)_{original}}\right) \qquad (1)\end{aligned}$$

where $n(H^+)$ is the molar concentration of H^+ in the air; $\Delta n(H^+)$ is the variation of $n(H^+)$. Considering that the $PM_{2.5}$ concentration was about 16.5 μg m^{-3} during the clean period, $\Delta n(H^+)$ can be evaluated as 16.5 μg m^{-3} multiplied by 1.0 nmol μg^{-1}, i.e., 16.5×10^{-9} mol m^{-3}. Assuming that the aerosol pH during the clean period is 1.0 and ALWC is 40.0 μg m^{-3} based on our observations, we can obtain that:

$$pH_{original} = -lg\frac{n(H^+)_{original}}{V(ALWC_{original})} = -lg\frac{n(H^+)_{original}}{\frac{40\ \mu g\cdot m^{-3}}{10^3\ kg\cdot m^{-3}}} = -lg\frac{n(H^+)_{original}}{4\times10^{-8}\ L\cdot m^{-3}} = 1.0$$

So, $n(H^+)_{original}$ is about 4×10^{-9} mol m^{-3}. According to Equation (1), ΔpH = lg(1+16.5/4) = 0.71. Therefore, an increase of 1.0 nmol μg^{-1} of $(2[SO_4^{2-}]+[NO_3^-])/PM_{2.5R}$ can cause a significant pH

variation of about 0.71. Thus, even though the difference of (2[SO_4^{2-}]+[NO_3^-])/$PM_{2.5R}$ levels between daytime and nighttime was visually small during clean (0.0010 μmol μg) and SP periods (0.0005 μmol μg), aerosol pH was very sensitive to it.

Comment (12): Line 255-256: "A decrease of 10% in RH resulted in a notable reduction of 7.6% in SOR and 7.2% in NOR (Figure 5)." How can the authors come to such a solid conclusion when the correlation here is not very high? What is the level of significance?

Response:

We calculated the level of significance about the correlations between RH and SOR and NOR. As shown in Figure 5, SOR was significantly correlated with RH when RH < 78% ($R = 0.64$, $p < 0.01$). NOR was also dependent on RH when RH < 75% ($R = 0.46$), but the level of significance was low ($p > 0.05$). So, we revised the relevant contents on lines 25–27 and 282–291 in the manuscript as follows:

"Furthermore, the oxidation rates of sulfur (SOR) ~~and nitrogen (NOR)~~ displayed a strong correlation with RH, particularly when RH was below 75%. A 10% increase in RH corresponded to a 7.6% rise in SOR ~~and a 7.2% elevation in NOR~~, which served as the primary driver of the higher aerosol acidity and $\%Fe_S$ at night."

"RH is a key factor in the formation of SO_4^{2-} and NO_3^- through heterogeneous/aqueous-phase reactions within aerosols (Wang et al., 2016; Liu et al., 2020; Hou et al., 2022). As demonstrated in Figure 5, the strong dependency of the oxidation rate of sulfur (SOR, defined as $[SO_4^{2-}]/([SO_4^{2-}] + [SO_2])$ on RH was observed under moderate humid conditions ($r = 0.64$, $p < 0.01$). But the nitrogen (NOR, defined as $[NO_3^-]/([NO_3^-] + [NO_2])$ had a poor dependence on RH ($r = 0.46$, $p > 0.05$). A decrease of 10% in RH resulted in a notable reduction of 7.6% in SOR (Figure 5). Such a striking RH dependence was observed mainly during the SP period, indicating the significant role of heterogeneous reactions in controlling the formation of SO_4^{2-}. Therefore, the facilitation of aqueous-phase conversions leading to the formation of SO_4^{2-} was more pronounced at night during the SP period, attributed to the high RH. This, in turn, resulted in a high proportion of SO_4^{2-} and acidic species, as well as the elevated SOR (Table 1, Figures 2b and S5). The nighttime aerosol pH was approximately 0.18 units lower than that during daytime, but this slight variation did not hinder the efficient formation of Fe_S during nighttime in SP periods."

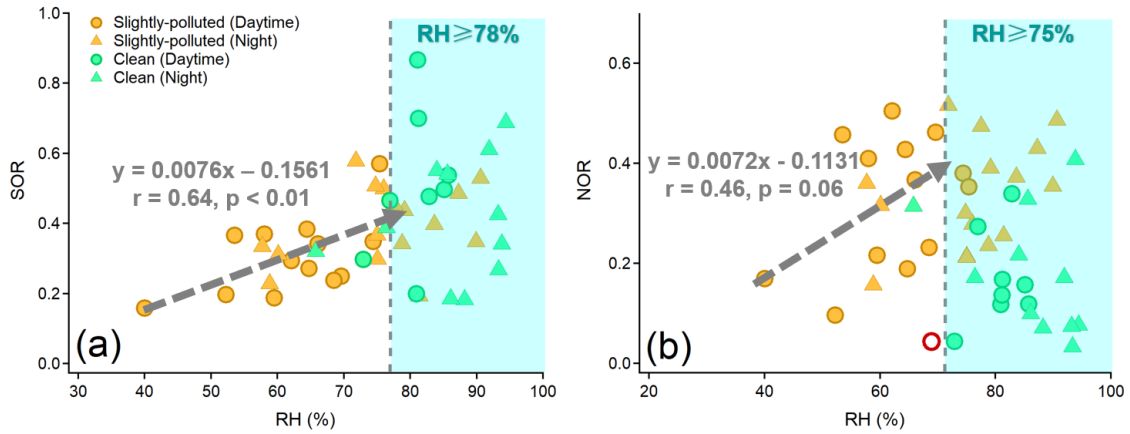

Figure 5: The dependence of SOR (a) and NOR (b) on RH during clean and slightly-polluted periods. The fitting of the regression line between SOR and RH was fitted when RH<78%. The fitting of the regression line between NOR and RH was fitted when RH<75% and one deviation point (the red circle in (b)) was removed.

Comment (13): Line 297: Figure 6 confused me. What are the different colors in the figure represent?

Response:

The color in Figure 6 stands for the level of SOR in a certain range of RH and O_X. We added color bars in Figure 6 and more descriptions in the figure caption. The revised figure is shown as follows:

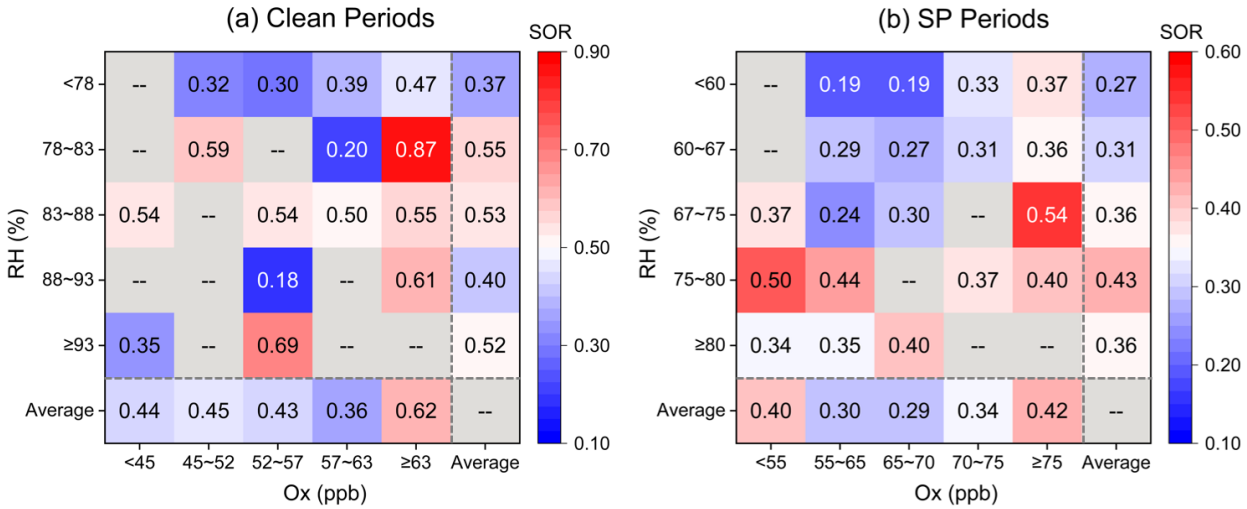

Figure 6: RH-O_x image plots colored by SOR during clean and SP periods. The last row and last column of the matrices represent the average value of SOR in the corresponding ranges of RH and O_x.

Comment (14): Line 316: For Figure 7, I believe the effect of oxalic acid on iron dissolution is important enough to suggest that the authors devote a chapter to the mechanism of oxalic acid and iron dissolution. In the current version, the authors did not do a good job of exploring the facilitating effect of oxalic acid on iron dissolution.

Response:

We devoted a chapter (Section 4.2.2) to the mechanisms of iron dissolution by oxalate promotion now, on lines 356–403 as follows:

4.2.2 The enhancement of $\%Fe_S$ promoted by oxalate-related conversions

Oxalate can form complexes with Fe(III) and participate in photochemical reactions through photoinduced charge transfer. Oxalate transfers its charge to the Fe(III) surface via photolytic reactions during daytime, resulting in the reduction of Fe(III) to Fe(II), followed by the dissociation of the formed Fe(II) from the surface and hence the dissolution of aerosol Fe (Zuo and Hoigne, 1992; Zhang et al., 2019; Lueder et al., 2020). Shi et al. (2022) identified the oxalate/Fe_T ratio as an excellent predictor for aerosol $\%Fe_S$ through machine learning, underscoring its remarkable effectiveness. However, field observations rarely confirm its influence on Fe_S from the perspective of oxalate-Fe photochemistry.

In this study, significant correlations were observed between $\%Fe_S$ and the molar ratio of [oxalate]/[Fe_T] during daytime in both clean periods (r = 0.82) and SP periods (r = 0.81) (Figure 8a and 8c). Similarly, a striking correlation was also found for nighttime during the SP period (r = 0.80, Figure 8d), although with a lower slope in the regression line (Figure 8). Noteworthy is the strong dependence of $\%Fe_S$ (or Fe_S) on oxalate concentration at night (Figures 8d, S6b and S6d). Field observations highlight the pivotal role of organic compound complexation in stabilizing Fe (Sakata et al., 2022). Additionally, as illustrated by Figures 8 and S6, the variation in $\%Fe_S$ induced by each unit variation in daytime [oxalate]/[Fe_T] was greater than its nighttime equivalent. The most notable increase was observed during the clean period, with a daytime slope of 13.8, marking a 1.6-fold increase over the SP period (daytime slope = 8.57). Similarly, the concentration of Fes per unit of oxalate showed a parallel trend, marking the highest daytime slope of the clean period during the campaign (Figure S6). Such patterns imply that enhanced sunlight in clear days may have catalyzed photochemical processes involving

daytime oxalate-Fe, leading to elevated concentrations of both Fes and %Fe_S. While these outcomes have only been discussed through laboratory simulations (Chen and Grassian, 2013), or indirectly by examining oxalate degradation or sulfate formation (Zhou et al. 2020), and they have been empirically discovered through field observations now in this study.

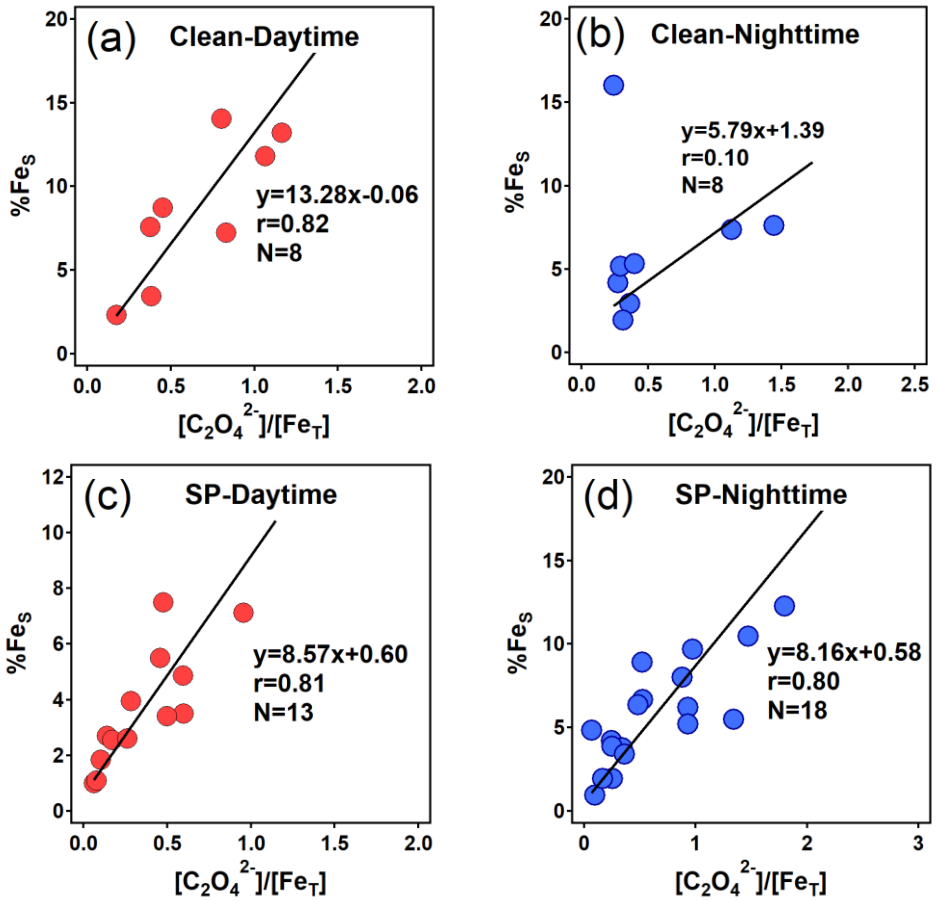

Figure 8: Relationships between %Fe_S and the molar ratio (unit: μmol μmol^{-1}) of oxalate to Fe_T during daytime and nighttime in clean and SP periods. An extreme point (marked by a pink triangle, %Fe_S = 37.2%) in (b) was removed.

Simultaneously, Fe_S species redox reactions can facilitate the formation of oxalate in return if the precursors are abundant, particularly with aqueous-phase reactions playing a pivotal role when RH exceeds 60% (Zhang et al., 2019). This may elucidate one of the main reasons behind the significant correlations observed between Fe_S and oxalate. Notably, oxalate concentration was higher during the daytime compared to the nighttime in this study (Figure S5), concomitant with elevated Fe_S concentrations. The photocatalytic degradation of oxalate-Fe, promoting Fe dissolution during daytime, was unlikely to be the predominant pathway influencing the oxalate concentration, otherwise a

decrease in oxalate concentration would occur (Dou et al., 2021). Therefore, the oxalate formation process catalyzed by Fe_S could yield a higher production rate of oxalate during the daytime than at night. Figure S7 portrays the conceptual diagram of these conversion processes. Similar scenarios might unfold for SO_4^{2-} formation due to the heightened Fe redox reactions during daytime (Zhou et al., 2020). Owing to the extremely low aerosol pH (< 2), transition-metal ions (TMIs, e.g., Fe_S)-catalyzed pathway could primarily influence the secondary formation of SO_4^{2-}, leading to potent aerosol acidity (Liu et al., 2021b). The escalated aerosol acidity, in turn, fostered the formation of Fe_S, thus furthering the generation of SO_4^{2-} and oxalate under high RH conditions. The resulting oxalate could then be complexed with Fe_S, sustaining $\%Fe_S$ at a high level at night.

To summarise, the findings of this study suggest that daytime photochemical processes indeed facilitated the dissolution of aerosol Fe, consequently elevating $\%Fe_S$ during the clean period. This mechanism, in turn, may foster the secondary formation of oxalate and SO_4^{2-}. The complexation of organic compounds significantly contributed to maintaining the high $\%Fe_S$ at night. While during SP periods, the diurnal variation in aerosol $\%Fe_S$ mainly resulted from the differing levels of aerosol acidity between daytime and nighttime, a conclusion strongly supported by the higher $\%Fe_S$ observed at night compared to daytime.

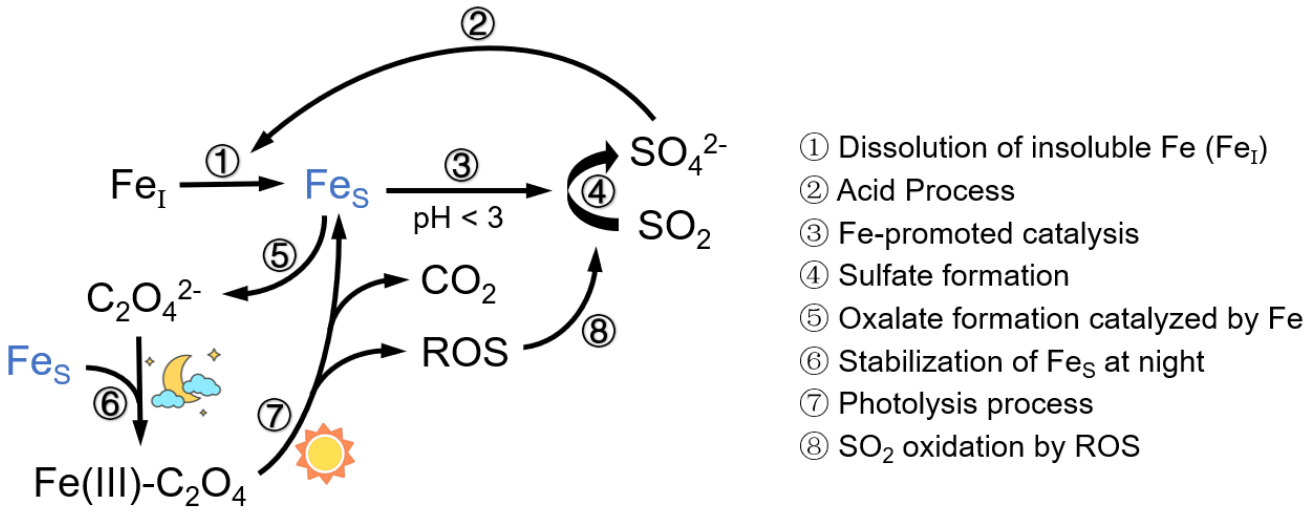

Figure S7: Conceptual diagram showing the Fe dissolution influenced by acid processes and oxalate.

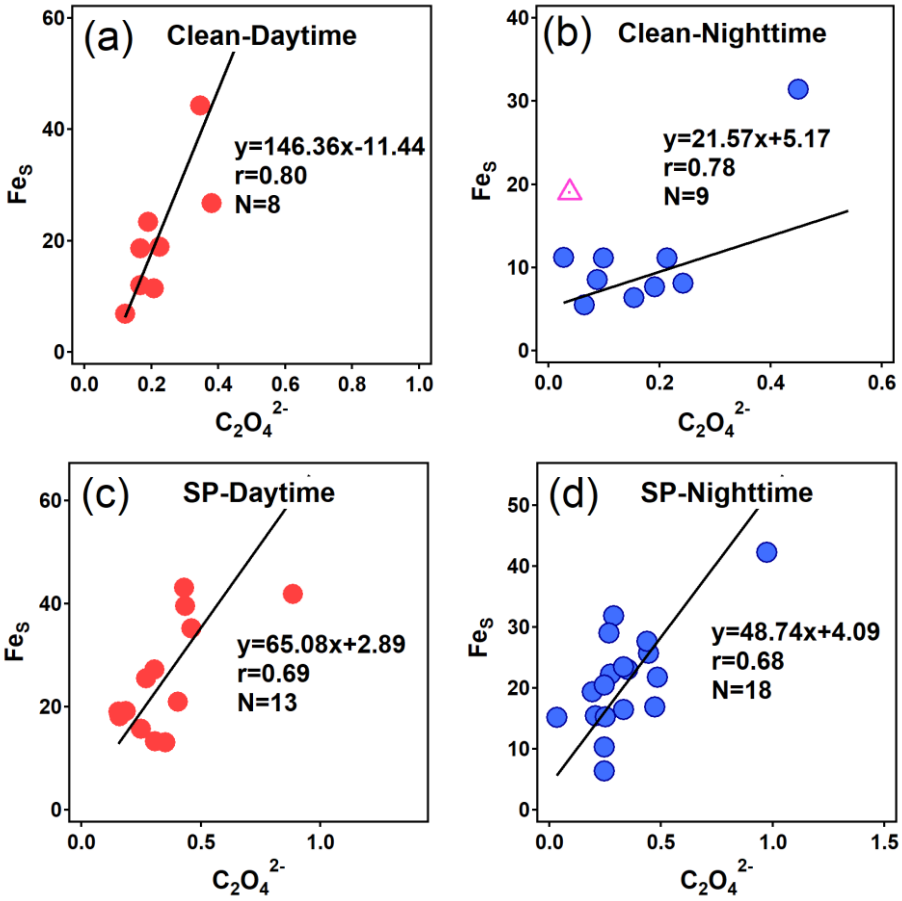

Figure S6: Relationships between soluble Fe (Fe_S, unit: ng m^{-3}) and oxalate (unit: µg m^{-3}). An extreme point (marked by a pink triangle, $\%Fe_S = 37.2\%$) in (b) was removed to obtain the more robust correlation coefficient.

References

Chen, H. and Grassian, V. H.: Iron Dissolution of Dust Source Materials during Simulated Acidic Processing: The Effect of Sulfuric, Acetic, and Oxalic Acids, Environ. Sci. Technol., 47, 10312–10321, 10.1021/es401285s, 2013.

Dou, J., Alpert, P. A., Corral Arroyo, P., Luo, B., Schneider, F., Xto, J., Huthwelker, T., Borca, C. N., Henzler, K. D., Raabe, J., Watts, B., Herrmann, H., Peter, T., Ammann, M., and Krieger, U. K.: Photochemical degradation of iron(III) citrate/citric acid aerosol quantified with the combination of three complementary experimental techniques and a kinetic process model, Atmos. Chem. Phys., 21, 315–338, 10.5194/acp-21-315-2021, 2021.

Liu, T., Chan, A. W. H., and Abbatt, J. P. D.: Multiphase Oxidation of Sulfur Dioxide in Aerosol

Particles: Implications for Sulfate Formation in Polluted Environments, Environ. Sci. Technol., 55, 4227–4242, 10.1021/acs.est.0c06496, 2021b.

Lueder, U., Jørgensen, B. B., Kappler, A., and Schmidt, C.: Photochemistry of iron in aquatic environments, Environmental Science: Processes & Impacts, 22, 12–24, 10.1039/C9EM00415G, 2020.

Sakata, K., Kurisu, M., Takeichi, Y., Sakaguchi, A., Tanimoto, H., Tamenori, Y., Matsuki, A., and Takahashi, Y.: Iron (Fe) speciation in size-fractionated aerosol particles in the Pacific Ocean: The role of organic complexation of Fe with humic-like substances in controlling Fe solubility, Atmos. Chem. Phys., 22, 9461–9482, 10.5194/acp-22-9461-2022, 2022.

Shi, J., Guan, Y., Gao, H., Yao, X., Wang, R., and Zhang, D.: Aerosol Iron Solubility Specification in the Global Marine Atmosphere with Machine Learning, Environ. Sci. Technol., 56, 16453–16461, 10.1021/acs.est.2c05266, 2022.

Zhang, G., Lin, Q., Peng, L., Yang, Y., Jiang, F., Liu, F., Song, W., Chen, D., Cai, Z., Bi, X., Miller, M., Tang, M., Huang, W., Wang, X., Peng, P. a., and Sheng, G.: Oxalate Formation Enhanced by Fe-Containing Particles and Environmental Implications, Environ. Sci. Technol., 53, 1269–1277, 10.1021/acs.est.8b05280, 2019.

Zhou, Y., Zhang, Y., Griffith, S. M., Wu, G., Li, L., Zhao, Y., Li, M., Zhou, Z., and Yu, J. Z.: Field Evidence of Fe-Mediated Photochemical Degradation of Oxalate and Subsequent Sulfate Formation Observed by Single Particle Mass Spectrometry, Environ. Sci. Technol., 54, 6562–6574, 10.1021/acs.est.0c00443, 2020.

Zuo, Y. and Hoigne, J.: Formation of hydrogen peroxide and depletion of oxalic acid in atmospheric water by photolysis of iron(III)-oxalato complexes, Environ. Sci. Technol., 26, 1014–1022, 10.1021/es00029a022, 1992.